*Bioscience, Biotechnology, and Biochemistry*, 2025, **89**, 398–405
https://doi.org/10.1093/bbb/zbae192
Advance access publication date: 10 December 2024
**Regular Paper**

# Angiogenin-catalyzed cleavage within tRNA anticodon-loops identified by cP-RNA-seq

Megumi Shigematsu[1,2], Ryuma Matsubara[1,2], Justin Gumas[1,2], Takuya Kawamura[1,2], and Yohei Kirino[1,2,*]

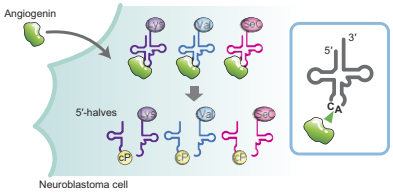
[1]Computational Medicine Center, Sidney Kimmel Medical College, Thomas Jefferson University, Philadelphia, PA, USA
[2]Department of Biochemistry and Molecular Biology, Sidney Kimmel Medical College, Thomas Jefferson University, Philadelphia, PA, USA
*Correspondence: Yohei Kirino, Yohei.Kirino@jefferson.edu

## Abstract

Angiogenin (Ang), an endoribonuclease belonging to the RNase A superfamily, cleaves the anticodon-loops of tRNAs to produce tRNA-half molecules. Although previous studies have demonstrated the involvement of Ang in the pathobiology of neurodegenerative disorders, the characterization of Ang-generated tRNA halves in neuronal cells remains limited. This is partly due to the technical limitations of standard RNA-seq methods, which cannot capture Ang-generated RNAs containing a 2′,3′-cyclic phosphate (cP). In this report, we established an Ang-treatment model using SH-SY5Y, a human neuroblastoma cell line, and demonstrated Ang-dependent accumulation of tRNA halves. By performing cP-RNA-seq, which selectively captures cP-containing RNAs, we identified Ang-generated tRNA halves and the specific cleavage positions within tRNA anticodon-loops responsible for their generation. Our results provide insights into the anticodon-loop cleavage and the selective production of a specific subset of tRNA halves by Ang.

**Keywords:** angiogenin, tRNA half, 2′,3′-cyclic phosphate, cP-RNA-seq

## Graphical abstract




In our established angiogenin treatment model using SH-SY5Y human neuroblastoma cells, cP-RNA-seq identified preferentially cleaved tRNA species and specific cleavage positions within anticodon-loops.

Transfer RNAs (tRNAs), the second most abundant cellular RNAs after ribosomal RNAs (rRNAs), function not only as adaptor molecules in translation but also as a source of short non-coding RNAs (sncRNAs). tRNA-derived sncRNAs play diverse roles beyond translation, and their regulation has been implicated in many human diseases (Anderson and Ivanov 2014; Kuhle, Chen and Schimmel 2023; Muthukumar *et al.* 2024). Among them, tRNA halves represent the most abundant subgroup. In mammalian cells, angiogenin (Ang), a member of the RNase A superfamily, is a major endoribonuclease responsible for cleaving tRNA anticodon-loops to produce tRNA halves (Fu *et al.* 2009; Yamasaki *et al.* 2009; Anderson and Ivanov 2014; Kuhle, Chen and Schimmel 2023; Muthukumar *et al.* 2024). Ang-catalyzed tRNA cleavage is triggered by a range of cellular stimuli, including various forms of stress (Fu *et al.* 2009; Yamasaki *et al.* 2009), sex hormone signaling pathways (Honda *et al.* 2015), and mycobacterial infections (Pawar *et al.* 2020). The resulting accumulation of tRNA halves has been shown to regulate translation (Ivanov *et al.* 2011), foster stress granule formation (Emara *et al.* 2010; Lyons *et al.* 2016), promote cell growth (Honda *et al.* 2015), and induce cytokine production in immune responses (Pawar *et al.* 2020; Gumas *et al.* 2024; Pawar, Kawamura and Kirino 2024; Shigematsu *et al.* 2024).

The RNase A superfamily enzymes employ acid-base catalysis for RNA cleavage, forming a 2′,3′-cyclic phosphate (cP) at the cleavage site (Thompson, Venegas and Raines 1994). While RNase A further hydrolyzes cP to form a 3′-monophosphate (P) as the final product, Ang, due to structural constraints in its catalytic site, cannot hydrolyze cP, leaving it at the 3′-end of 5′-tRNA halves (Shigematsu, Kawamura and Kirino 2018). Standard RNA-seq methods, widely used in sncRNA sequencing studies, cannot capture these cP-containing RNAs (cP-RNAs), as the 3′-adaptor (AD) cannot ligate to a cP end. Consequently, 5′-tRNA halves and other cP-RNAs are significantly underrepresented in RNA-seq data, leading to their understudied status in the cellular transcriptome (Shigematsu, Kawamura and Kirino 2018; Shigematsu and Kirino 2022). To overcome this limitation, we developed cP-RNA-seq (Honda *et al.* 2015; Honda, Morichika and Kirino 2016), a specialized method for selectively sequencing cP-RNAs, including 5′-tRNA halves, and applied it to characterizing the short cP-RNAome in various cells and tissues (Honda *et al.* 2017;

**Received:** 23 October 2024; **Accepted:** 2 December 2024
© The Author(s) 2024. Published by Oxford University Press on behalf of Japan Society for Bioscience, Biotechnology, and Agrochemistry. This is an Open Access article distributed under the terms of the Creative Commons Attribution-NonCommercial License (https://creativecommons.org/licenses/by-nc/4.0/), which permits non-commercial re-use, distribution, and reproduction in any medium, provided the original work is properly cited. For commercial re-use, please contact journals.permissions@oup.com

Shigematsu *et al.* 2019; Pawar *et al.* 2020; Shigematsu and Kirino 2020; Shigematsu *et al.* 2021).

Ang was initially discovered as a factor promoting angiogenesis (Fett *et al.* 1985), but recent studies have increasingly highlighted its role in various other fields including neurobiology. Genetic evidence links Ang to neurodegenerative disorders, including Parkinson's disease and amyotrophic lateral sclerosis, with over 30 distinct mutations involving amino acid changes in the *ANG* gene identified in patients (Greenway *et al.* 2006; Corrado *et al.* 2007; Wu *et al.* 2007; Conforti *et al.* 2008; Gellera *et al.* 2008; Paubel *et al.* 2008; Fernandez-Santiago *et al.* 2009; Luigetti *et al.* 2011; van Es *et al.* 2011; Padhi *et al.* 2012; Zou *et al.* 2012). Some of these mutations have been shown to alter Ang's ribonucleolytic activity, either reducing or enhancing it (Wu *et al.* 2007; Thiyagarajan *et al.* 2012; Bradshaw *et al.* 2017). Ang exhibits a neuroprotective effect on neurons; the addition of recombinant Ang to neuronal cell cultures increases cell survival or reduces cell death under specific stressors or neurotoxin treatments (Kieran *et al.* 2008; Steidinger *et al.* 2011; Hoang *et al.* 2019). While these findings underscore Ang's importance in neuronal physiology, the involvement of its ribonuclease activity and tRNA-half generation in these processes remains poorly understood. Although a few RNA-seq studies have identified tRNA-derived sncRNAs produced in an Ang-dependent manner, no studies have applied cP-RNA-seq or T4 PNK-seq, where RNA is treated with T4 polynucleotide kinase (T4 PNK) prior of AD ligation (Giraldez *et al.* 2019; Gumas *et al.* 2024; Shigematsu *et al.* 2024), to appropriately capture cP-containing 5′-tRNA halves in cells treated with Ang.

The RNase A superfamily commonly cleaves at the 3′-side of pyrimidines, with a stronger preference for cytidine (C) over uridine (U) (Raines 1998). Ang exhibits the highest preference for cleaving between 5′-C and A-3′, followed by 5′-C–G-3′ (Russo *et al.* 1996). Despite well-documented substrate specificity in dinucleotides, Ang's cleavage patterns in actual tRNA anticodon-loops remain poorly characterized, partly due to the limitations of standard RNA-seq methods in detecting cP-containing RNAs produced by Ang. In this study, we used the widely used human neuroblastoma cell line, SH-SY5Y, and demonstrated that recombinant Ang is taken up by the cells, where it cleaves tRNA anticodon-loops to produce tRNA halves. We performed cP-RNA-seq to identify the primary products of tRNA cleavage by Ang and characterized preferential cleavage sites.

# Materials and methods

## Bacterial strains and human cell line

*Escherichia coli* strain HST08, provided as Stellar Competent cells (TaKaRa), was used for all cloning experiments. For protein expression, BL21 (DE3) Star (Thermo Fisher Scientific) was used.

The human neuroblastoma cell line SH-SY5Y was obtained from ATCC (CRL-2266). For treatment, recombinant Ang was added to the culture medium at 1 μg/mL. The cells were collected by trypsinization to remove residual Ang attached to the cell surface.

## Purification of recombinant Ang

The coding region of human *ANG* gene starting from glutamine at position 25 was cloned into the pGEX-6P-2 vector with or without a C-terminal 2× FLAG tag. The QuikChange II Site-Directed Mutagenesis Kit (Agilent) was used to introduce point mutations. The plasmid was transformed into BL21 (DE3) Star. Cells were grown in 1.2 L of LB (Luria-Bertani) medium containing 100 μg/mL ampicillin at 25 °C. When the $OD_{600}$ reached 0.5, protein expression was induced with 0.5 mM isopropyl-$\beta$-D-1-thiogalactopyranoside (IPTG), and the culture was continued for 6 h. The cells were collected by centrifugation and stored at –80 °C until purification. For purification, the cells were resuspended in lysis buffer (50 mM Tris-HCl pH 8.0, 500 mM NaCl, 1 mM PMSF, and 1 mM EDTA), and lysed by sonication on ice for 4 min (30% amplitude, 15 s intervals). The lysate was cleared by centrifugation at 20 000 ×*g* at 4 °C for 30 min. The supernatant was subjected to affinity chromatography using Glutathione Sepharose 4B (Cytiva). After 1 h of binding at 4 °C, the beads were washed with lysis buffer without PMSF four times, followed by a wash with PreScission buffer (50 mM Tris-HCl pH 7.5, 150 mM NaCl, 1 mM EDTA, and 1 mM DTT). PreScission protease (Cytiva) was added to the beads, and the mixture was incubated at 4 °C overnight. The supernatant was collected as the elution fraction and concentrated using Vivaspin 3kMWCO filtration unit (Sartorius) to ∼600 μL. The fraction was further subjected to size exclusion chromatography using Superdex 200 10/300 GL (Cytiva). The column was equilibrated with GFC buffer (50 mM Tris-HCl pH 8.0, 200 mM NaCl, and 1 mM DTT). Elution fractions containing protein of the expected size were pooled and concentrated using Vivaspin. The purified proteins were stored in storage buffer (50 mM Tris-HCl pH 8.0, 20 mM NaCl, 1 mM DTT, and 40% (v/v) glycerol) at –30 °C. Protein purity was evaluated by NuPAGE, followed by CBB staining.

## *In vitro* RNA cleavage assay

Total RNA extracted from HeLa cells was used to test the ribonuclease activity of Ang in either of two assay buffers: biochemically optimal buffer (50 mM MES pH 5.5, 10 mM NaCl, 10 mM $MgCl_2$, and 0.1 mg/mL BSA) or physiological buffer (50 mM Tris-HCl pH 7.5, 100 mM NaCl, 10 mM $MgCl_2$, and 0.1 mg/mL BSA). After incubation of the RNA with recombinant Ang, proteinase K solution (0.5 mg/mL Proteinase K, 50 mM Tris-HCl pH 8.0, 4 mM EDTA, 75 mM NaCl, 0.05% SDS, and 0.5% Triton X-100) was added to the reaction mixture and incubated at 37 °C for 1 min. An equal volume of 2× LS (7 M urea, 1× TBE, 0.025% BPB, and 0.025% XC) was then added, and the RNA was analyzed by denaturing polyacrylamide gel electrophoresis (PAGE) containing 7 M urea, followed by SYBR Gold staining. When synthetic $tRNA^{HisGUG}$ was used as a substrate, the RNA was first synthesized *in vitro* as described previously (Shigematsu and Kirino 2017) and then 5′-end labeled with $^{32}P$. The magnesium concentration of the assay buffers was adjusted to 20 mM or varied as indicated. The $^{32}P$ signal was detected using a Typhoon phosphorimager (Cytiva).

## Western blot

SH-SY5Y cells were resuspended in RSB-200 buffer (20 mM Tris-HCl pH 7.5, 150 mM NaCl, and 2.5 mM $MgCl_2$) containing 0.5% Triton X-100 and 0.1% Nonidet P-40, and lysed by brief sonication. The supernatant was subjected to 12% NuPAGE using 1× MES running buffer, followed by transfer to a nitrocellulose membrane. Target proteins were detected using the following antibodies: anti-FLAG M2 antibody (1:1000, Sigma-Aldrich), anti-GAPDH antibody (1:5 000, Proteintech), and anti-Histone H2A antibody (1:2000, Cell Signaling Technology).

## Norther blot

Northern blot was performed as described previously (Shigematsu and Kirino 2020) using an antisense probe (5′-GTCTCATGCTCTACCGACTG-3′) specific for the 5′-$tRNA^{LysCUU}$ half.

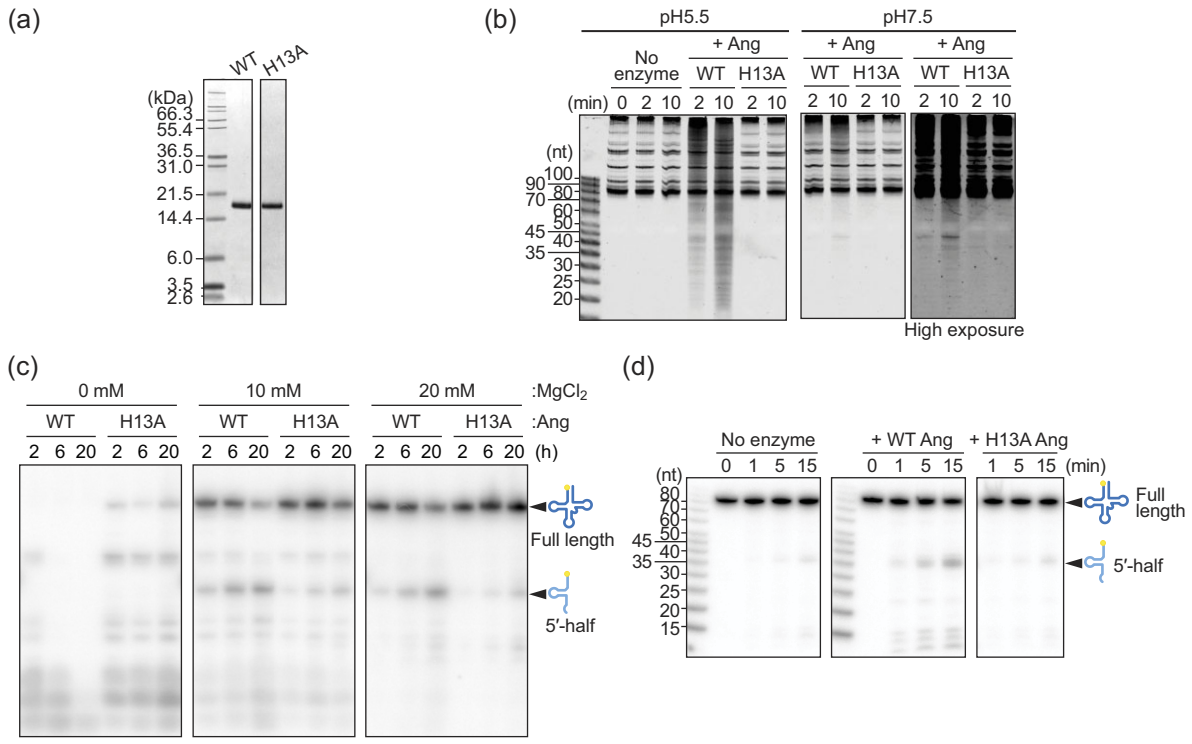



**Figure 1.** *In vitro* anticodon cleavage by recombinant Ang. (a) Purified recombinant Ang, visualized by CBB staining. (b) Ribonuclease activity of recombinant Ang on total RNA extracted from HeLa cells. HeLa total RNA (100 ng/μL) was incubated with 2.5 μM Ang in physiological buffer at 37 °C. Cleaved RNAs were analyzed by denaturing PAGE and visualized by SYBR Gold staining. Single-stranded DNA was used as a size marker. (c and d) Ribonuclease activity of recombinant Ang on $^{32}$P-labeled synthetic tRNA$^{HisGUG}$. The tRNA was incubated with 2.5 μM Ang at 37 °C in either physiological buffer (c) or in biochemically optimal buffer (d).

## TaqMan RT-qPCR

TaqMan-based reverse transcription quantitative PCR (RT-qPCR) for specific quantification of 5′-tRNA halves were performed as previously described (Shigematsu and Kirino 2020). The sequences of the primers and TaqMan probes used are shown in Table S1.

## cP-RNA-seq and bioinformatics

cP-RNA-seq and bioinformatics analyses of the obtained reads were performed as described previously (Honda *et al.* 2015; Honda, Morichika, and Kirino 2016; Shigematsu *et al.* 2019; Pawar *et al.* 2020; Shigematsu and Kirino 2020; Shigematsu *et al.* 2021). Briefly, ~20-50-nucleotides (nt) RNAs were gel-purified from SH-SY5Y total RNA and treated with calf intestinal alkaline phosphatase (New England Biolabs). After phenol-chloroform purification, the RNAs were oxidized by incubation in 10 mM $NaIO_4$ at 0 °C for 40 min in the dark, followed by ethanol precipitation. The RNAs were then treated with T4 PNK (New England Biolabs). After phenol-chloroform purification, directional ligation of ADs, cDNA generation, and PCR amplification were performed using the TruSeq Small RNA Library Preparation Kit (Illumina). The amplified cDNAs were sequenced on NextSeq 500 using SR75 flowcell at the MetaOmics Core Facility of the Sidney Kimmel Cancer Center at Thomas Jefferson University. Original FASTQ files were quality-filtered using Cutadapt, and reads of 20-50 nt in length were mapped onto human tRNAs obtained from the Genomic tRNA Database, release 18 (Chan and Lowe 2009; Chan and Lowe 2016).

# Results and discussion

## Recombinant human Ang produces tRNA halves *in vitro*

We purified recombinant human Ang from *E. coli*, obtaining both the wild-type (WT) protein and an H13A mutant in which histidine at position 13, a residue in the catalytic triad (H13, K40, and H114) (Shapiro, Riordan and Vallee 1986), was replaced with alanine (Figure 1a and Figure S1). The WT Ang showed substantial *in vitro* RNA cleavage activity when incubated with HeLa total RNA, while the H13A mutant exhibited significantly reduced activity as expected (Figure 1b). Consistent with the reports that Ang displays high-ribonucleolytic activity under low-pH conditions (Shapiro, Riordan and Vallee 1986; Lee and Vallee 1989), the WT Ang demonstrated stronger RNA cleavage activity at pH 5.5 compared to pH 7.5 (Figure 1b). When 5′-$^{32}$P-labeled mature tRNA$^{HisGUG}$ was used as a substrate, recombinant ANG-mediated cleavage produced a 5′-tRNA$^{HisGUG}$ half in the presence of magnesium (Figure 1c). In contrast, the absence of magnesium in the reaction led to rapid degradation at various positions of tRNA$^{HisGUG}$ (Figure 1c). Although the RNase A superfamily relies on catalytic amino acids for proton transfer and does not require magnesium ions for catalysis, magnesium is essential for mature tRNA to form its proper L-shaped tertiary structure (Xu, MacKerell and Nilsson 2016; Schauss *et al.* 2021), which is necessary for Ang to cleave the anticodon-loop. Supporting the need for proper tertiary structure, most 3′-tRNA halves generated by Ang-mediated cleavage retain their attached amino acid (Honda *et al.* 2015), suggesting that Ang cleaves aminoacylated mature tRNAs complexed with an elongation factor. Moreover, Ang-mediated cleavage in the

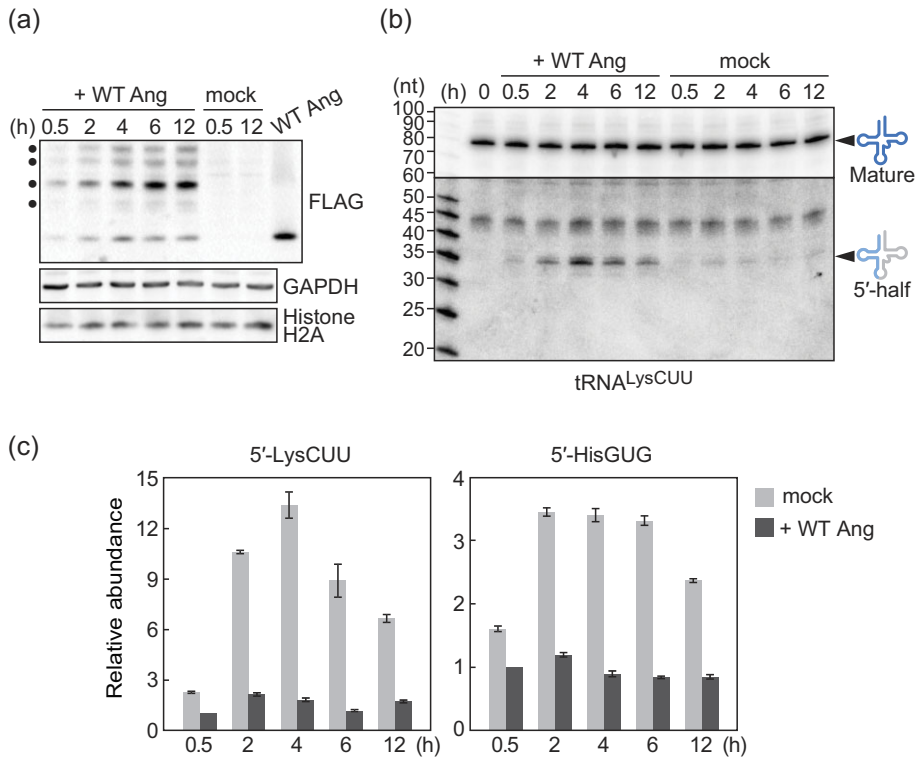



**Figure 2.** Ang is taken up by SH-SY5Y cells where it produces 5′-tRNA halves. (a) SH-SY5Y cells were treated with 1 μg/mL of recombinant Ang, and the uptake of the protein was monitored by western blot targeting its FLAG tag. Bands at higher molecular weights are indicated by black dots. GAPDH and Histone H2A were analyzed as controls. (b) The levels of mature $tRNA^{LysCUU}$ and 5′-LysCUU were analyzed by northern blot. (c) The levels of 5′-LysCUU and 5′-HisGUG were quantified by TaqMan RT-qPCR. Expression levels were normalized to 5S rRNA and are shown as relative abundance, with the mock treatment at 0.5 h set to 1. Error bars represent standard deviation (S.D.) from technical replicates.

ribosomal A-site (Loveland *et al.* 2024) further supports that Ang targets properly folded, aminoacylated, and elongation factor-bound tRNAs. In the presence of magnesium, the reaction using mature tRNA as a substrate mainly yielded a 5′-tRNA half not only under physiological conditions with neutral pH and modest salt concentration (Figure 1c) but also under biochemically optimal conditions, where lower pH and salt concentration induce faster Ang-mediated cleavage (Figure 1d).

## Ang produces tRNA halves in SH-SY5Y cells

We next characterized the activity of recombinant Ang in SH-SY5Y cells. The RNase A superfamily, to which Ang belongs, comprises secretory proteins that are taken up by recipient cells (Russo, Acharya and Shapiro 2001). Upon addition of recombinant Ang to the culture medium, we observed its incorporation into cells beginning at 30 min post-treatment, and the highest accumulation of ANG inside the cells was detected 4 h after the treatment (Figure 2a). In addition to the band of the recombinant Ang, multiple bands appeared gradually in higher molecular weight regions, whose band intensities were higher in longer treatments (Figure 2a). The intensity of these higher bands appeared to be dependent on the dose of recombinant Ang added to the medium (Figure S2). We speculate that these higher bands with a ladder-like appearance may represent ubiquitinated Ang, although Ang's cellular dynamics have not been well studied. To investigate Ang-induced tRNA-half expression, we performed a northern blot for the 5′-half of $tRNA^{LysCUU}$ (5′-LysCUU). As shown in Figure 2b, 5′-LysCUU exhibited the highest accumulation at 4 h post-treatment, while the levels of mature $tRNA^{LysCUU}$ remained unchanged by Ang treatment. This peak in the tRNA half accumulation coincides with the peak levels of Ang, but not with the presumably ubiquitinated, higher molecular weight forms of Ang, which show greater accumulation at 6 and 12 h post-treatment (Figure 2a). This suggests that the higher molecular weight protein may not be active in tRNA cleavage. We further confirmed the Ang-induced accumulation of tRNA halves using TaqMan RT-qPCR specifically designed for tRNA half quantification (Honda *et al.* 2015; Kawamura, Shigematsu and Kirino 2022). Consistent with the northern blot result, 5′-LysCUU showed the highest accumulation at 4 h post-treatment (Figure 2c). In contrast, 5′-HisGUG exhibited a more modest fold change upon Ang treatment, achieving its peak accumulation at 2 h and maintaining this level until 6 h. The differences between these two 5′-tRNA halves may reflect Ang's substrate preference in cleavage and/or the distinct stability and turnover rate of each tRNA half species in the cells.

## Characterization of Ang-produced tRNA halves in SH-SY5Y cells using cP-RNA-seq

We next aimed to sequence the tRNA halves produced by Ang treatment in SH-SY5Y cells using cP-RNA-seq (Honda *et al.* 2015; Honda, Morichika, and Kirino 2016). Because cP-RNA-seq specifically sequences RNAs containing a cP and does not capture RNAs with a P and hydroxyl group (OH) at their 3′-ends (Figure 3a), it is expected to fully identify Ang-generated cP-containing 5′-tRNA halves while omitting other fragments generated by secondary cleavage from other ribonucleases. We treated SH-SY5Y cells for 4 h with either WT Ang or a triple mutant in which all three catalysts (H13, K40, and H114) were replaced with alanine (Figure S1). The ribonuclease activity of the triple mutant has been confirmed to be null (Figure S3). cP-RNA-seq using RNAs extracted

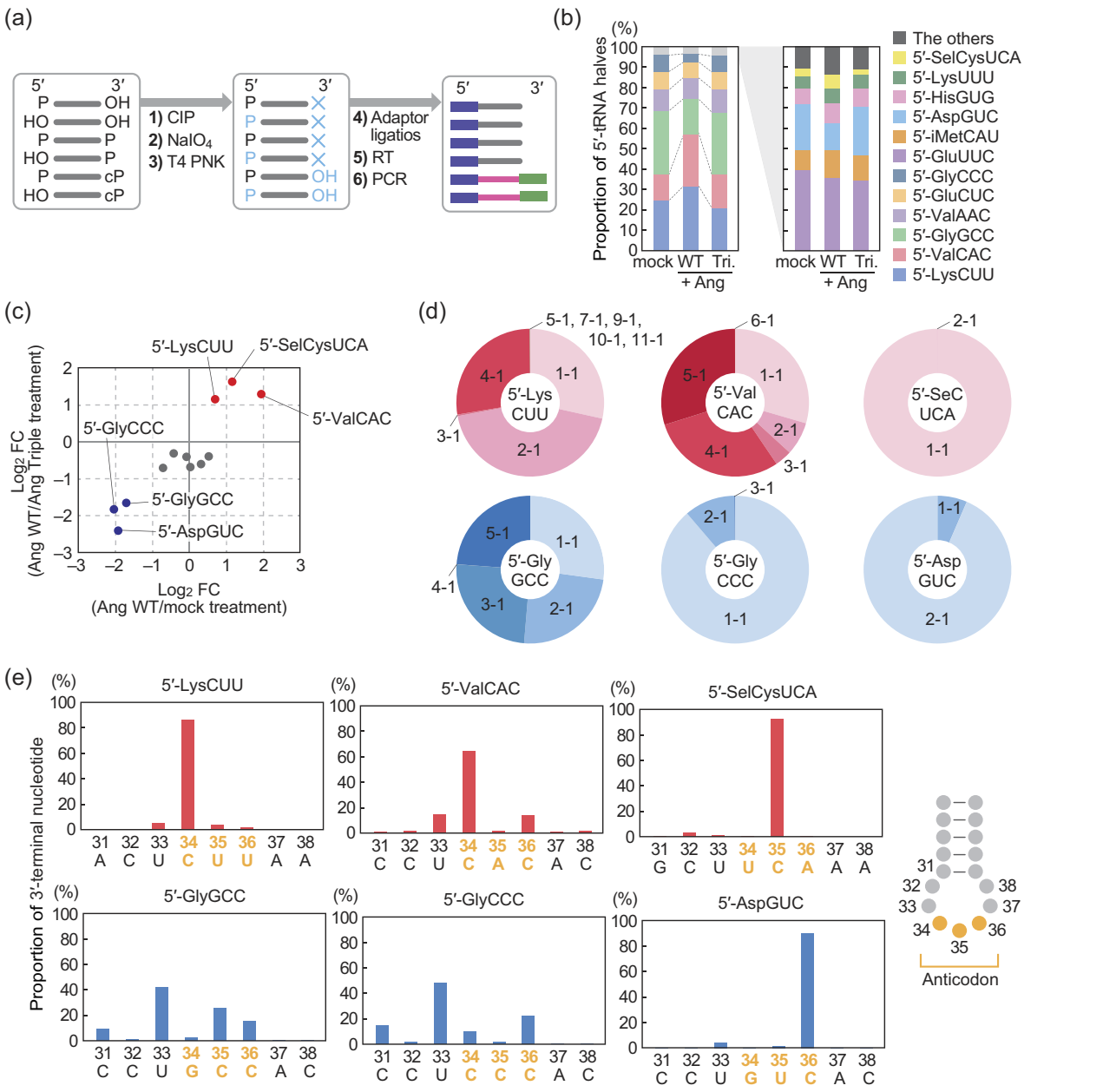



**Figure 3.** cP-RNA-seq for Ang-produced 5′-tRNA halves. (a) Schematic representation of cP-RNA-seq. (b) Proportion of each 5′-tRNA half species. The top 12 most abundant species are indicated. (c) The top 12 most abundant 5′-tRNA halves from (b) are plotted against their $\log_2$ fold changes, calculated from reads per million. Dots in the first quadrant indicate 5′-tRNA halves that were consistently upregulated by WT Ang treatment compared to mock and triple mutant treatments. Dots in the third quadrant indicate 5′-tRNA halves that were consistently downregulated in WT Ang treatment. (d) Isodecoders producing the six up- or downregulated 5′-tRNA halves shown in (c) in WT Ang-treated sample. (e) Ratio of 3′-terminal positions for each 5′-tRNA half in WT Ang-treated sample.

from the cells yielded abundant 5′-tRNA half reads. As observed in cP-RNA-seq libraries from other cells and tissues (Honda *et al.* 2015; Shigematsu *et al.* 2019; Pawar *et al.* 2020; Shigematsu and Kirino 2020; Shigematsu *et al.* 2021), the identified 5′-tRNA halves were derived from a focused subset of cytoplasmic tRNA isoacceptors (Figure 3b). Specifically, $tRNA^{LysCUU}$, $tRNA^{ValCAC}$, $tRNA^{GlyGCC}$, $tRNA^{ValAAC}$, $tRNA^{GluCUC}$, and $tRNA^{GlyCCC}$ collectively accounted for over 95% of the identified 5′-tRNA halves. By comparing the relative ratios of the reads between samples treated with WT Ang and mock-treated control, as well as between those treated with WT Ang and with a triple mutant Ang, we found that three 5′-tRNA halves, 5′-LysCUU, 5′-ValCAC, and 5′-SelCysCUA, were the most consistently upregulated species following WT Ang treatment (Figure 3c). In contrast, the relative ratios of 5′-GlyGCC, 5′-GlyCCC, and 5′-AspGUC were consistently downregulated (Figure 3c). It should be noted that these comparisons are based on changes in the proportion of read numbers within each library but not standardized read numbers, thus not reflecting absolute quantitative differences between samples. Indeed, our previous study demonstrated the production of 5′-AspGUC by Ang (Honda *et al.* 2015), suggesting that even the three downregulated species are produced upon Ang treatment. Nevertheless, these results

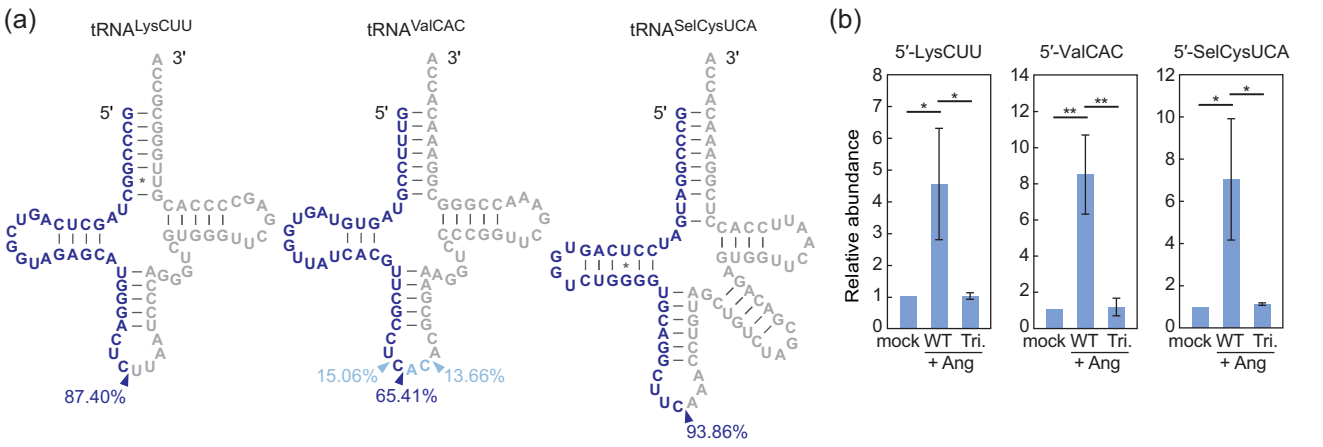



**Figure 4.** 5′-LysCUU, 5′-ValCAC, and 5′-SelCysUCA are produced by Ang in SH-SY5Y cells. (a) Cloverleaf structures of $tRNA^{LysCUU}$, $tRNA^{ValCAC}$, and $tRNA^{SelCysUCA}$. Ang cleavage positions for the generation of 5′-tRNA halves are indicated by arrowheads. The proportions shown are from WT Ang-treated sample. The quantified 5′-tRNA halves are highlighted. (b) SH-SY5Y cells treated with Ang for 4 h were subjected to TaqMan RT-qPCR. Expression levels were normalized to 5S rRNA and are presented as relative abundance, with the mock treatment set to 1. For multiple comparison, we performed Analysis of Variance (ANOVA) followed by the Tukey-Kramer HSD test. The ANOVA results yielded $p$-values of 0.0078, 0.0006, and 0.0068, respectively (from left to right). *$P < 0.05$ and **$P < 0.01$, by Tukey's test. No significant differences were observed between the mock and triple mutant treatments for any of the three targets ($P > 0.5$).

suggest that Ang exhibits cleavage preferences, preferentially producing the three upregulated species, while tRNAs corresponding to the three downregulated species are less favored substrates for Ang.

## Ang preferentially cleaves at the 3′-side of cytidine on the 5′-side of the anticodon-loops

Further analysis focusing on the three upregulated and three downregulated 5′-tRNA half species revealed that they were produced from specific isodecoders (Figure 3d and Figure S4). We predicted the Ang-mediated cleavage sites within the anticodon-loop based on the 3′-terminal nucleotide positions of the identified 5′-tRNA halves. All three upregulated species were predominantly generated by cleavage at the 3′-side of a cytidine residue. Specifically, 5′-LysCUU was produced by cleavage between C34 and U35, while 5′-ValCAC and 5′-SelCysUCA resulted from cleavage between C and A (Figures 3e and 4a). For 5′-ValCAC, cleavage occurred between C34 and A35, U33 and C36, and C36 and A37; for 5′-SelCysUCA, cleavage occurred between C35 and A36. These findings align with previous reports showing that Ang has a strong cleavage preference for the 3′-side of pyrimidines, particularly with the highest catalysis observed between the 5′-C and A-3′ sequence (Russo *et al.* 1996). Interestingly, although the C–A site is also present in 5′-GlyGCC and 5′-GlyCCC at C36 and A37, their primary Ang-mediated cleavage occurs at U33 and G/C34. A previous study demonstrated that Ang activity toward U-G and U-C is over 90-fold lower than its activity toward C-A (Russo *et al.* 1996). In addition, 5′-AspGUC was predominantly produced by cleavage between C36 and A37 but showed the most downregulation when comparing WT and triple mutant ANG-treated samples (Figure 3c). Collectively, these results suggest that Ang preferentially cleaves the C-A sequence located on the 5′-side of the second anticodon nucleotide, while cleavage efficiency decreases for C-A sequences located on the 3′-side of the anticodon-loop.

To confirm the preferential cleavage of Ang for the three upregulated 5′-tRNA halves (Figure 4a) in SH-SY5Y cells, we treated the cells with Ang and quantified their levels by TaqMan RT-qPCR. Treatment with WT Ang resulted in a significant upregulation of all three 5′-tRNA halves, whereas the triple mutant Ang treatment showed levels comparable to the mock treatment (Figure 4b), confirming that Ang robustly generates these tRNA halves.

## Conclusion

We utilized cP-RNA-seq to specifically capture Ang-generated, cP-containing 5′-tRNA halves, providing insights into Ang's substrate preferences in endoribonucleolytic activity and the generation of specific tRNA half species. It is likely that Ang preferentially cleaves the 5′-side of the anticodon-loop, which may indicate structural recognition of substrate tRNA by Ang. Further biochemical and structural characterizations are required to fully elucidate the molecular mechanisms underlying Ang-mediated tRNA cleavage. Treatment of SH-SY5Y cells with Ang successfully demonstrated the accumulation of tRNA halves, providing a platform for investigating the functional roles of Ang and its generated tRNA halves in a neuronal context. This model facilitates exploration of their impacts on key neuronal processes, including differentiation, maintenance of the dopaminergic phenotype, and calcium signaling dynamics. The diverse Ang mutants identified in patients with neurodegenerative disorders present an intriguing research avenue. Investigating how these mutants alter tRNA half profiles in neuronal cells could provide critical insights into disease mechanisms. Introducing recombinant Ang or its generated tRNA halves into cellular and animal models of neurodegenerative diseases offers a straightforward approach to elucidate the direct influence of these sncRNAs on disease pathobiology. This line of research could potentially bridge the gap between molecular mechanisms and clinical manifestations, paving the way for novel therapeutic strategies targeting Ang-mediated tRNA processing in neurodegenerative diseases.

## Supplementary material

Supplementary material is available at *Bioscience, Biotechnology, and Biochemistry* online.

## Data availability

The cP-RNA-seq dataset generated in this study is publicly available at the NCBI's Sequence Read Archive under BioProject PRJNA1175680. The unique identifiers of the 5′-tRNA halves investigated are summarized in Table S2.

## Author contribution

The research was conceived by M.S. and Y.K. The experiments were designed by M.S. and Y.K., and performed by M.S., R.M., J.G., and T.K. Data analysis was performed by M.S. The manuscript was written by M.S. and Y.K., with contributions from J.G. Funding support was provided by M.S. and Y.K.

## Funding

This study was supported in part by National Institutes of Health grants (GM106047, HL150560, HL175371, AI168975, and AI171366 to Y.K.), American Lung Association Catalyst Award Grant (CA935540 to M.S.), and JSPS Postdoctoral Fellowship for Research Abroad (to M.S.). This research utilized the MetaOmics Core Facility at the Sidney Kimmel Comprehensive Cancer Center at Thomas Jefferson University and was supported by the National Institutes of Health Grant (P30CA056036).

## Disclosure statement

No potential conflict of interest was reported by the authors.

## Acknowledgments

We are grateful to Dr. Ryusuke Suzuki (Cedars-Sinai Medical Center) for technical assistance.

## References

Anderson P, Ivanov P. tRNA fragments in human health and disease. *FEBS Lett* 2014;**588**:4297-304. https://doi.org/10.1016/j.febslet.2014.09.001.

Bradshaw WJ, Rehman S, Pham TT *et al.* Structural insights into human angiogenin variants implicated in Parkinson's disease and amyotrophic lateral sclerosis. *Sci Rep* 2017;**7**:41996. https://doi.org/10.1038/srep41996.

Chan PP, Lowe TM. GtRNAdb: a database of transfer RNA genes detected in genomic sequence. *Nucleic Acids Res* 2009;**37**:D93-7. https://doi.org/10.1093/nar/gkn787.

Chan PP, Lowe TM. GtRNAdb 2.0: an expanded database of transfer RNA genes identified in complete and draft genomes. *Nucleic Acids Res* 2016;**44**:D184-9. https://doi.org/10.1093/nar/gkv1309.

Conforti FL, Sprovieri T, Mazzei R *et al.* A novel angiogenin gene mutation in a sporadic patient with amyotrophic lateral sclerosis from southern Italy. *Neuromuscul Disord* 2008;**18**:68-70. https://doi.org/10.1016/j.nmd.2007.07.003.

Corrado L, Battistini S, Penco S *et al.* Variations in the coding and regulatory sequences of the angiogenin (ANG) gene are not associated to ALS (amyotrophic lateral sclerosis) in the Italian population. *J Neurol Sci* 2007;**258**:123-7. https://doi.org/10.1016/j.jns.2007.03.009.

Emara MM, Ivanov P, Hickman T *et al.* Angiogenin-induced tRNA-derived stress-induced RNAs promote stress-induced stress granule assembly. *J Biol Chem* 2010;**285**:10959-68. https://doi.org/10.1074/jbc.M109.077560.

Fernandez-Santiago R, Hoenig S, Lichtner P *et al.* Identification of novel Angiogenin (ANG) gene missense variants in German patients with amyotrophic lateral sclerosis. *J Neurol* 2009;**256**:1337-42. https://doi.org/10.1007/s00415-009-5124-4.

Fett JW, Strydom DJ, Lobb RR *et al.* Isolation and characterization of angiogenin, an angiogenic protein from human carcinoma cells. *Biochemistry* 1985;**24**:5480-6. https://doi.org/10.1021/bi00341a030.

Fu H, Feng J, Liu Q *et al.* Stress induces tRNA cleavage by angiogenin in mammalian cells. *FEBS Lett* 2009;**583**:437-42. https://doi.org/10.1016/j.febslet.2008.12.043.

Gellera C, Colombrita C, Ticozzi N *et al.* Identification of new ANG gene mutations in a large cohort of Italian patients with amyotrophic lateral sclerosis. *Neurogenetics* 2008;**9**:33-40. https://doi.org/10.1007/s10048-007-0111-3.

Giraldez MD, Spengler RM, Etheridge A *et al.* Phospho-RNA-seq: a modified small RNA-seq method that reveals circulating mRNA and lncRNA fragments as potential biomarkers in human plasma. *EMBO J* 2019;**38**:e101695. https://doi.org/10.15252/embj.2019101695.

Greenway MJ, Andersen PM, Russ C *et al.* ANG mutations segregate with familial and 'sporadic' amyotrophic lateral sclerosis. *Nat Genet* 2006;**38**:411-3. https://doi.org/10.1038/ng1742.

Gumas J, Kawamura T, Shigematsu M, Kirino Y. Immunostimulatory short non-coding RNAs in the circulation of patients with tuberculosis infection. *Mol Ther Nucleic Acids* 2024;**35**:102156. https://doi.org/10.1016/j.omtn.2024.102156.

Hoang TT, Johnson DA, Raines RT, Johnson JA. Angiogenin activates the astrocytic Nrf2/antioxidant-response element pathway and thereby protects murine neurons from oxidative stress. *J Biol Chem* 2019;**294**:15095-103. https://doi.org/10.1074/jbc.RA119.008491.

Honda S, Kawamura T, Loher P *et al.* The biogenesis pathway of tRNA-derived piRNAs in Bombyx germ cells. *Nucleic Acids Res* 2017;**45**:9108-20. https://doi.org/10.1093/nar/gkx537.

Honda S, Loher P, Shigematsu M *et al.* Sex hormone-dependent tRNA halves enhance cell proliferation in breast and prostate cancers. *Proc Natl Acad Sci USA* 2015;**112**:E3816-25. https://doi.org/10.1073/pnas.1510077112.

Honda S, Morichika K, Kirino Y. Selective amplification and sequencing of cyclic phosphate-containing RNAs by the cP-RNA-seq method. *Nat Protoc* 2016;**11**:476-89. https://doi.org/10.1038/nprot.2016.025.

Ivanov P, Emara MM, Villen J *et al.* Angiogenin-induced tRNA fragments inhibit translation initiation. *Mol Cell* 2011;**43**:613-23. https://doi.org/10.1016/j.molcel.2011.06.022.

Kawamura T, Shigematsu M, Kirino Y. *In vitro* production and multiplex quantification of 2',3'-cyclic phosphate-containing 5'-tRNA half molecules. *Methods* 2022;**203**:335-41. https://doi.org/10.1016/j.ymeth.2021.04.024.

Kieran D, Sebastia J, Greenway MJ *et al.* Control of motoneuron survival by angiogenin. *J Neurosci* 2008;**28**:14056-61. https://doi.org/10.1523/JNEUROSCI.3399-08.2008.

Kuhle B, Chen Q, Schimmel P. tRNA renovatio: rebirth through fragmentation. *Mol Cell* 2023;**83**:3953-71. https://doi.org/10.1016/j.molcel.2023.09.016.

Lee FS, Vallee BL. Characterization of ribonucleolytic activity of angiogenin towards tRNA. *Biochem Biophys Res Commun* 1989;**161**:121-6. https://doi.org/10.1016/0006-291X(89)91569-6.

Loveland AB, Koh CS, Ganesan R *et al.* Structural mechanism of angiogenin activation by the ribosome. *Nature* 2024;**630**:769-76. https://doi.org/10.1038/s41586-024-07508-8.

Luigetti M, Lattante S, Zollino M *et al.* SOD1 G93D sporadic amyotrophic lateral sclerosis (SALS) patient with rapid progression

and concomitant novel ANG variant. *Neurobiol Aging* 2011;**32**:1924 e15-8. https://doi.org/10.1016/j.neurobiolaging.2011.04.004.

Lyons SM, Achorn C, Kedersha NL *et al.* YB-1 regulates tiRNA-induced stress granule formation but not translational repression. *Nucleic Acids Res* 2016;**44**:6949-60. https://doi.org/10.1093/nar/gkw418.

Muthukumar S, Li CT, Liu RJ *et al.* Roles and regulation of tRNA-derived small RNAs in animals. *Nat Rev Mol Cell Biol* 2024;**25**:359-78. https://doi.org/10.1038/s41580-023-00690-z.

Padhi AK, Kumar H, Vasaikar SV *et al.* Mechanisms of loss of functions of human angiogenin variants implicated in amyotrophic lateral sclerosis. *PLoS One* 2012;**7**:e32479. https://doi.org/10.1371/journal.pone.0032479.

Paubel A, Violette J, Amy M *et al.* Mutations of the ANG gene in French patients with sporadic amyotrophic lateral sclerosis. *Arch Neurol* 2008;**65**:1333-6. https://doi.org/10.1001/archneur.65.10.1333.

Pawar K, Kawamura T, Kirino Y. The tRNA(Val) half: a strong endogenous toll-like receptor 7 ligand with a 5'-terminal universal sequence signature. *Proc Natl Acad Sci USA* 2024;**121**:e2319569121. https://doi.org/10.1073/pnas.2319569121.

Pawar K, Shigematsu M, Sharbati S, Kirino Y. Infection-induced 5'-half molecules of tRNAHisGUG activate toll-like receptor 7. *PLoS Biol* 2020;**18**:e3000982. https://doi.org/10.1371/journal.pbio.3000982.

Raines RT. Ribonuclease A. *Chem Rev* 1998;**98**:1045-66. https://doi.org/10.1021/cr960427h.

Russo A, Acharya KR, Shapiro R. Small molecule inhibitors of RNase A and related enzymes. *Methods Enzymol* 2001;**341**:629-48. https://doi.org/10.1016/S0076-6879(01)41181-5.

Russo N, Acharya KR, Vallee BL, Shapiro R. A combined kinetic and modeling study of the catalytic center subsites of human angiogenin. *Proc Natl Acad Sci USA* 1996;**93**:804-8. https://doi.org/10.1073/pnas.93.2.804.

Schauss J, Kundu A, Fingerhut BP, Elsaesser T. Magnesium contact ions stabilize the tertiary structure of transfer RNA: electrostatics mapped by two-dimensional infrared spectra and theoretical simulations. *J Phys Chem B* 2021;**125**:740-7. https://doi.org/10.1021/acs.jpcb.0c08966.

Shapiro R, Riordan JF, Vallee BL. Characteristic ribonucleolytic activity of human angiogenin. *Biochemistry* 1986;**25**:3527-32. https://doi.org/10.1021/bi00360a008.

Shigematsu M, Kawamura T, Deshpande DA, Kirino Y. Immunoactive signatures of circulating tRNA- and rRNA-derived RNAs in chronic obstructive pulmonary disease. *Mol Ther Nucleic Acids* 2024;**35**:102285. https://doi.org/10.1016/j.omtn.2024.102285.

Shigematsu M, Kawamura T, Kirino Y. Generation of 2',3'-cyclic phosphate-containing RNAs as a hidden layer of the transcriptome. *Front Genet* 2018;**9**:562. https://doi.org/10.3389/fgene.2018.00562.

Shigematsu M, Kawamura T, Morichika K *et al.* RNase kappa promotes robust piRNA production by generating 2',3'-cyclic phosphate-containing precursors. *Nat Commun* 2021;**12**:4498. https://doi.org/10.1038/s41467-021-24681-w.

Shigematsu M, Kirino Y. 5'-Terminal nucleotide variations in human cytoplasmic tRNAHisGUG and its 5'-halves. *RNA* 2017;**23**:161-8. https://doi.org/10.1261/rna.058024.116.

Shigematsu M, Kirino Y. Oxidative stress enhances the expression of 2',3'-cyclic phosphate-containing RNAs. *RNA Biol* 2020;**17**:1060-9. https://doi.org/10.1080/15476286.2020.1766861.

Shigematsu M, Kirino Y. Making invisible RNA visible: discriminative sequencing methods for RNA molecules with specific terminal formations. *Biomolecules* 2022;**12**:611. https://doi.org/10.3390/biom12050611.

Shigematsu M, Morichika K, Kawamura T *et al.* Genome-wide identification of short 2',3'-cyclic phosphate-containing RNAs and their regulation in aging. *PLoS Genet* 2019;**15**:e1008469. https://doi.org/10.1371/journal.pgen.1008469.

Steidinger TU, Standaert DG, Yacoubian TA. A neuroprotective role for angiogenin in models of Parkinson's disease. *J Neurochem* 2011;**116**:334-41. https://doi.org/10.1111/j.1471-4159.2010.07112.x.

Thiyagarajan N, Ferguson R, Subramanian V, Acharya KR. Structural and molecular insights into the mechanism of action of human angiogenin-ALS variants in neurons. *Nat Commun* 2012;**3**:1121. https://doi.org/10.1038/ncomms2126.

Thompson JE, Venegas FD, Raines RT. Energetics of catalysis by ribonucleases: fate of the 2',3'-cyclic phosphodiester intermediate. *Biochemistry* 1994;**33**:7408-14. https://doi.org/10.1021/bi00189a047.

Van Es MA, Schelhaas HJ, Van Vught PW *et al.* Angiogenin variants in Parkinson disease and amyotrophic lateral sclerosis. *Ann Neurol* 2011;**70**:964-73. https://doi.org/10.1002/ana.22611.

Wu D, Yu W, Kishikawa H *et al.* Angiogenin loss-of-function mutations in amyotrophic lateral sclerosis. *Ann Neurol* 2007;**62**:609-17. https://doi.org/10.1002/ana.21221.

Xu Y, MacKerell AD, Jr., Nilsson L. Structural effects of modified ribonucleotides and magnesium in transfer RNAs. *Bioorg Med Chem* 2016;**24**:4826-34. https://doi.org/10.1016/j.bmc.2016.06.037.

Yamasaki S, Ivanov P, Hu GF, Anderson P. Angiogenin cleaves tRNA and promotes stress-induced translational repression. *J Cell Biol* 2009;**185**:35-42. https://doi.org/10.1083/jcb.200811106.

Zou ZY, Wang XN, Liu MS *et al.* Identification of a novel missense mutation in angiogenin in a Chinese amyotrophic lateral sclerosis cohort. *Amyotroph Lateral Scler* 2012;**13**:270-5. https://doi.org/10.3109/17482968.2011.643900.

**Received:** 23 October 2024. **Accepted:** 2 December 2024

© The Author(s) 2024. Published by Oxford University Press on behalf of Japan Society for Bioscience, Biotechnology, and Agrochemistry. This is an Open Access article distributed under the terms of the Creative Commons Attribution-NonCommercial License (https://creativecommons.org/licenses/by-nc/4.0/), which permits non-commercial re-use, distribution, and reproduction in any medium, provided the original work is properly cited. For commercial re-use, please contact journals.permissions@oup.com